JBC RESEARCH ARTICLE

HSP90AB1 is a host factor that promotes porcine deltacoronavirus replication

Received for publication, April 13, 2023, and in revised form, November 22, 2023 Published, Papers in Press, December 12, 2023,
https://doi.org/10.1016/j.jbc.2023.105536

Yujia Zhao[1,2], Jianlin Yuan[1], Dai Xiao[1], Luwen Zhang[1], Cheng Li[1], Jingfei Hu[1], Rui Chen[1], Daili Song[1], Yiping Wen[1], Rui Wu[1], Qin Zhao[1], Senyan Du[1], Qigui Yan[1], Xinfeng Han[1], Xintian Wen[1], Sanjie Cao[1,3,4], and Xiaobo Huang[1,3,4,*]

From the [1]Research Center for Swine Diseases, College of Veterinary Medicine, Sichuan Agricultural University, Chengdu, China; [2]Laboratory Animal Center, Zunyi Medical University, Zunyi, China; [3]Sichuan Science-Observation Experiment Station for Veterinary Drugs and Veterinary Diagnostic Technology, Ministry of Agriculture, Chengdu, China; [4]National Animal Experiments Teaching Demonstration Center, Sichuan Agricultural University, Chengdu, China

Reviewed by members of the JBC Editorial Board. Edited by Ursula Jakob

Porcine deltacoronavirus (PDCoV) is an emerging enteropathogenic coronavirus. It causes mortality in neonatal piglets and is of growing concern because of its broad host range, including humans. To date, the mechanism of PDCoV infection remains poorly understood. Here, based on a genome-wide CRISPR screen of PDCoV-infected cells, we found that HSP90AB1 (heat shock protein 90 alpha family class B1) promotes PDCoV infection. Knockdown or KO of *HSP90AB1* in LLC-PK cells resulted in a significantly suppressed PDCoV infection. Infected cells treated with HSP90 inhibitors 17-AAG and VER-82576 also showed a significantly suppressed PDCoV infection, although KW-2478, which does not affect the ATPase activity of HSP90AB1, had no effect on PDCoV infection. We found that HSP90AB1 interacts with the N, NS7, and NSP10 proteins of PDCoV. We further evaluated the interaction between N and HSP90AB1 and found that the C-tail domain of the N protein is the HSP90AB1-interacting domain. Further studies showed that HSP90AB1 protects N protein from degradation *via* the proteasome pathway. In summary, our results reveal a key role for HSP90AB1 in the mechanism of PDCoV infection and contribute to provide new host targets for PDCoV antiviral research.

Porcine deltacoronavirus (PDCoV) was first reported in Hong Kong in 2012 and is currently widespread in pig populations in Asia and the Americas (1, 2). In piglets, it causes severe diarrhea, vomiting, and dehydration, resulting in very high mortality rates (3). PDCoV can also infect adult pigs (4), cattle (5), mice (6), chicks, and turkey poults (7), and recently, PDCoV infections have been reported in Haitian children (8).

It is widely accepted that some host factors play a role in viral entry and replication (9), and that virus–host interactions are key to viral pathogenesis (10). For example, porcine aminopeptidase N (APN) plays an important role in PDCoV entry (11), although it remains controversial whether APN is the critical functional receptor for PDCoV infection (12, 13). PDCoV can enter host cells *via* the endocytic pathway and initiate a successful infection (14). Fang *et al.* (15) reported that PDCoV entry into IPI-2I cells depends on clathrin and dynamin, and that Rab5 and Rab7 are involved in regulating PDCoV endocytosis. Ji *et al.* (16) showed that cholesterol contributes to PDCoV entry, and Ke *et al.* (17) showed that cholesterol 25-hydroxylase suppresses PDCoV entry by regulating cholesterol metabolism. Signal transducer and activator of transcription 1 interacts with PDCoV and inhibits viral internalization (18), whereas transmembrane protein 41B (TMEM41B) is required for coronavirus replication (19).

CRISPR genome-wide screening has been used to identify host factors essential for human coronavirus infection, such as severe acute respiratory syndrome coronavirus 2 (SARS-CoV-2) (20, 21), SARS-CoV (20), middle east respiratory syndrome coronavirus (MERS-CoV) (22, 23), human coronavirus 229E (23, 24), and human coronavirus OC43 (25). For porcine coronaviruses, Luo *et al.* (26) found that zinc finger DHHC-type palmitoyltransferase 17 affects viral genome replication during swine acute diarrhea syndrome coronavirus (SADS-CoV) infection, and Tse *et al.* (27) reported that KO of placenta-associated eight results in a reduction of SADS-CoV subgenomic RNA expression. TMEM41B is a host factor required for transmissible gastroenteritis virus (TGEV) replication and contributes to the formation of coronavirus replication organelles (19). To date though, there are no genome-wide screening studies that directly identify porcine genes required for PDCoV infection.

To explore the host factors involved in PDCoV infection, we performed a CRISPR genome-wide screening in PDCoV-infected LLC-PK cells and found that single-guide RNAs (sgRNAs) targeting *CPSF2*, *HSP90AB1*, *SLC27A4*, *CCDC124*, *TOMM6*, *EDIL3*, *SLC9A5*, and *DCTN1* were the most enriched candidate genes. Further analysis indicated that HSP90AB1 (heat shock protein 90 alpha family class B1) was the top-hit host factor using MAGeCK algorithm method. Then, we systematically identified the function of HSP90AB1 during PDCoV infection and found HSP90AB1 promotes PDCoV infection at the postentry stage. Among the PDCoV proteins, HSP90AB1 interacts with nucleocapsid (N) protein and is involved in maintaining N protein stability to prevent its

* For correspondence: Xiaobo Huang, rsghb110@126.com.

degradation *via* the proteasome pathway. Our findings provided new insights into the mechanisms of PDCoV–host interactions and will contribute to providing new host targets for PDCoV antiviral research.

Results

CRISPR screening identified host factors associated with PDCoV infection

To identify host factors involved in PDCoV infection, a genome-wide CRISPR screening in LLC-PK cells was performed; the overall screening strategy is illustrated in Figure 1*A*. Briefly, LLC-PK-Cas9 (lentivirus expressing Cas9 protein) cell lines were generated by transducing LLC-PK WT cells with LLC-PK-Cas9. LLC-PK-Cas9 cells were transduced with lentivirus containing a porcine genome-wide sgRNA library (which encodes 89,796 sgRNAs targeting 30,410 annotated protein-coding genes). Transduced cells were selected with puromycin for 7 days. Puromycin-resistant cells were infected with PDCoV. PDCoV-resistant cells were expanded and harvested to isolate genomic DNA for Illumina sequencing to determine the enrichment of the sgRNAs using the MAGeCK algorithm (28). Sequencing analysis results showed that sgRNAs targeting *CPSF2*, *HSP90AB1*, *SLC27A4*, *CCDC124*, *TOMM6*, *EDIL3*, *SLC9A5*, and *DCTN1* were the most enriched. Using the MAGeCK algorithm, *HSP90AB1* was the top-hit host factor and was selected for further analysis (Fig. 1, *B* and *C*). HSP90 is known to be involved in MERS-CoV and SARS-CoV-2 infection where it helps stabilize the viral N protein (29, 30), that it also regulates SARS-CoV-2 infection *via* binding viral RNA (31), that inhibition of HSP90 by 17-AAG reduces SARS-CoV and SARS-CoV-2 infection (29), and that HSP90AA1 is a host factor for SARS-CoV-2 infection in human cell lines (32). Therefore, we chose the host factor HSP90AB1 for further experiments.

HSP90AB1 enhances PDCoV infection

To validate the CRISPR hit gene, we generated HSP90AB1 knockdown (KD) cells (designated HSP90AB1^{KD}) for PDCoV infection. The detail of HSP90AB1^{KD} cell generation is shown in the Supporting information section. As shown in Fig. S1, *A* and *B*, KD of HSP90AB1 resulted in a 75% reduction in the level of *HSP90AB1* mRNA and a 62% decrease in HSP90AB1 levels. From PDCoV-infected WT and KD cells, quantitative RT–PCR (qRT–PCR) for *M* mRNA revealed that, except at 3 hpi, levels were significantly different throughout the infection time course (6, 12, 18, and 24 hpi); *M* mRNA levels were lower by 95, 84, 80, and 75%, respectively, in KD cells (Fig. S1*C*). The levels of N protein and viral titers in supernatant were also significantly decreased in KD cells, as revealed by Western blot and $TCTD_{50}$, respectively (Fig. S1, *D* and *E*). To further determine the role of HSP90AB1 in PDCoV infection, HSP90AB1^{KO} cells were used to assess the contribution of HSP90AB1 to PDCoV infection. The KO cell line was verified by qRT–PCR and Western blot. The results showed that *HSP90AB1* mRNA and protein were barely detectable in KO cells (Fig. 2, *A* and *B*). By Cell Counting Kit-8 (CCK-8) assay,

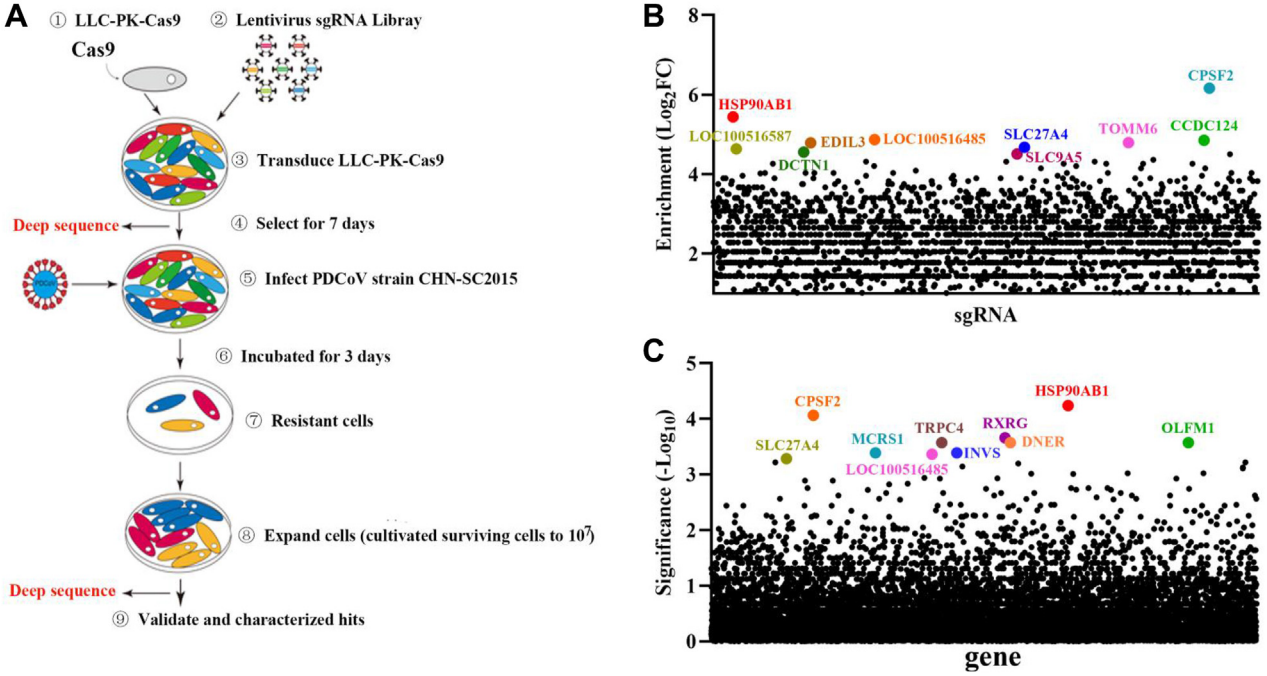

Figure 1. CRISPR screening reveals host factor HSP90AB1 is associated with PDCoV infection. *A*, schematic overview of the genome-wide CRISPR screen in LLC-PK cells. LLC-PK cells expressing Cas9 were transduced with lentiviruses encoding a pig CRISPR KO pooled sgRNA library at an MOI of 0.3. At 2 days post-transduction, cells were selected with puromycin (4 μg/ml) for 7 days and subsequently infected with PDCoV at an MOI of 0.04. PDCoV-resistant cells were expanded and harvested to isolate genomic DNA (gDNA) for Illumina sequencing. *B* and *C*, candidate genes identified by the CRISPR screening. *B*, data analysis was performed by using the MAGeCK method to identify enriched sgRNA. *C*, the corresponding genes were rank ordered by robust rank aggregation (RRA) scores. HSP90AB1, heat shock protein 90 alpha family class B1; MOI, multiplicity of infection; PDCoV, porcine deltacoronavirus; sgRNA, single-guide RNA.

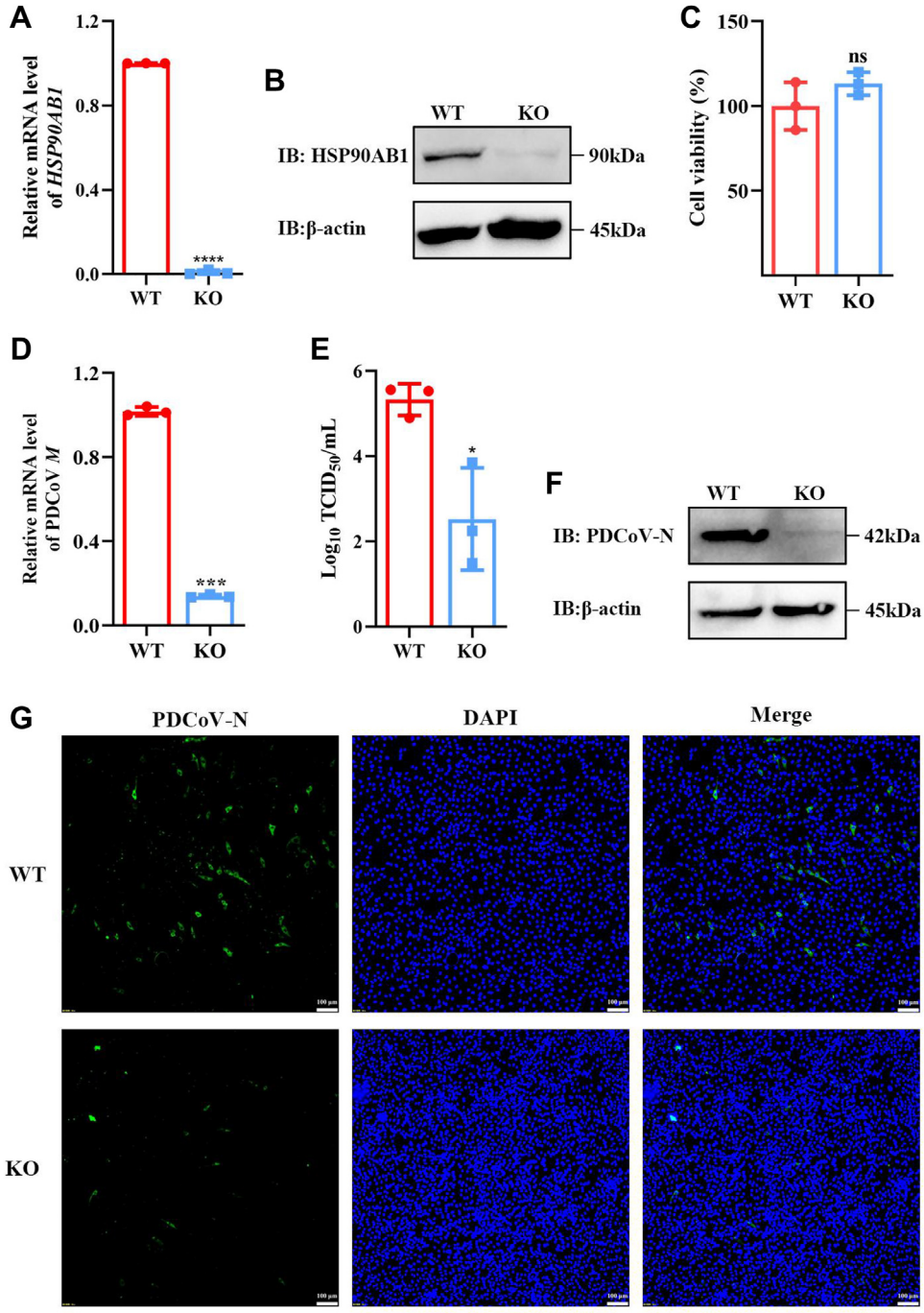

Figure 2. KO of HSP90AB1 suppresses PDCoV infection. *A*, qRT–PCR of *HSP90AB1* mRNA and (*B*) protein levels in WT and KO cells. *C*, cell viability of WT and KO cells was evaluated by CCK-8 assay. *D*, PDCoV *M* mRNA levels and (*E*) viral titers in the cell supernatants at 24 hpi. *F*, N protein levels in WT and KO cells. *G*, IFA of PDCoV-infected WT and KO cells. Viral N protein was stained with FITC-anti-rabbit IgG (*green*), and nuclei were stained with DAPI (*blue*). Magnification = 10×, scale bar represents 100 μm. Data are shown as the mean ± SD from three independent experiments. CCK-8, Cell Counting Kit-8; DAPI, 4′,6-diamidino-2-phenylindole; HSP90AB1, heat shock protein 90 alpha family class B1; IFA, immunofluorescence assay; IgG, immunoglobulin G; PDCoV, porcine deltacoronavirus; qRT–PCR, quantitative RT–PCR.

there was no significant difference in the viability of KO cells compared with WT (Fig. 2*C*). As shown in Figure 2*D*, KO of HSP90AB1 resulted in significantly a lower level (∼85%) of *M* mRNA, and viral titers were reduced by approximately 2.8 Log_{10} $TCID_{50}$/ml (Fig. 2*E*). Western blot and immunofluorescence assay results also showed a significantly decreased level of N protein compared with that in WT cells (Fig. 2, *F* and *G*). These results demonstrate that KO of *HSP90AB1* significantly reduces PDCoV infection.

LLC-PK and ST cells were transfected with pEGFP-N1-HSP90AB1, and HSP90AB1 protein levels were detected by Western blot. Results showed that a weak band measuring 120 kDa was observed when using a GFP as the primary antibody in LLC-PK cells. However, no band at 120 kDa was

observed when using an HSP90AB1 as the primary antibody. However, in ST cells, a band at 120 and 90 kDa, as determined by Western blot analysis, using HSP90AB1 as the primary antibody (Fig. 3, *A* and *B*), indicating exogenous expression of HSP90AB1 was only detected in ST cells. Then, the transfected ST cells were used to evaluate the effect of HSP90AB1 overexpression on PDCoV infection, and results found that it had no significant effect on viral infection (Fig. 3, *C–E*). These findings indicated that HSP90AB1 plays a relevant role in PDCoV infection.

HSP90AB1 ATPase activity is required for PDCoV infection

LLC-PK cells were treated with the following inhibitors: 17-AAG (targets HSP90AA1 and HSP90AB1), VER-82576 (targets only HSP90AB1), and KW-2478 (binds HSP90AA1 with high affinity). The effect of these inhibitors on PDCoV infection in LLC-PK cells was evaluated *in vitro*. By CCK-8 assay, there was no significant degradation of cell viability in cells treated with 20 μM or less 17-AAG or KW-2478 (Fig. S2, *A* and *B*), and there was no significant degradation of cell viability in cells treated with VER-82576 at 1.0 μM (Fig. S2*C*). A schematic of the infection and inhibitor treatment time course is illustrated in Figure 4*A*. Cells infected in the presence of 5, 10, or 20 μM 17-AAG had 75, 90, and 99%, respectively, lower levels of *M* mRNA than untreated cells (Fig. 4*B*). Those infected in the presence of 250, 500, or 1000 nM VER-82576 had 20, 56, and 70%, respectively, lower levels of *M* mRNA (Fig. 4*E*). $TCID_{50}$ and Western blot analysis results showed that 17-AAG (Fig. 4, *C* and *D*) and VER-82576 (Fig. 4, *F* and *G*) had a significant inhibitory effect on PDCoV infection in a dose-dependent manner, but KW-2478 had no significant inhibitory effect on PDCoV infection (Fig. 4, *H–J*). These results show that it is HSP90AB1, not HSP90AA1, that affects PDCoV infection. qRT–PCR and Western blot analysis showed that neither 17-AAG (Fig. S3, *A* and *B*) nor VER-82576 (Fig. S3, *C* and *D*) had effect on *HSP90AB1* mRNA or protein levels. Likewise, neither 17-AAG (Fig. S3, *E* and *F*) nor

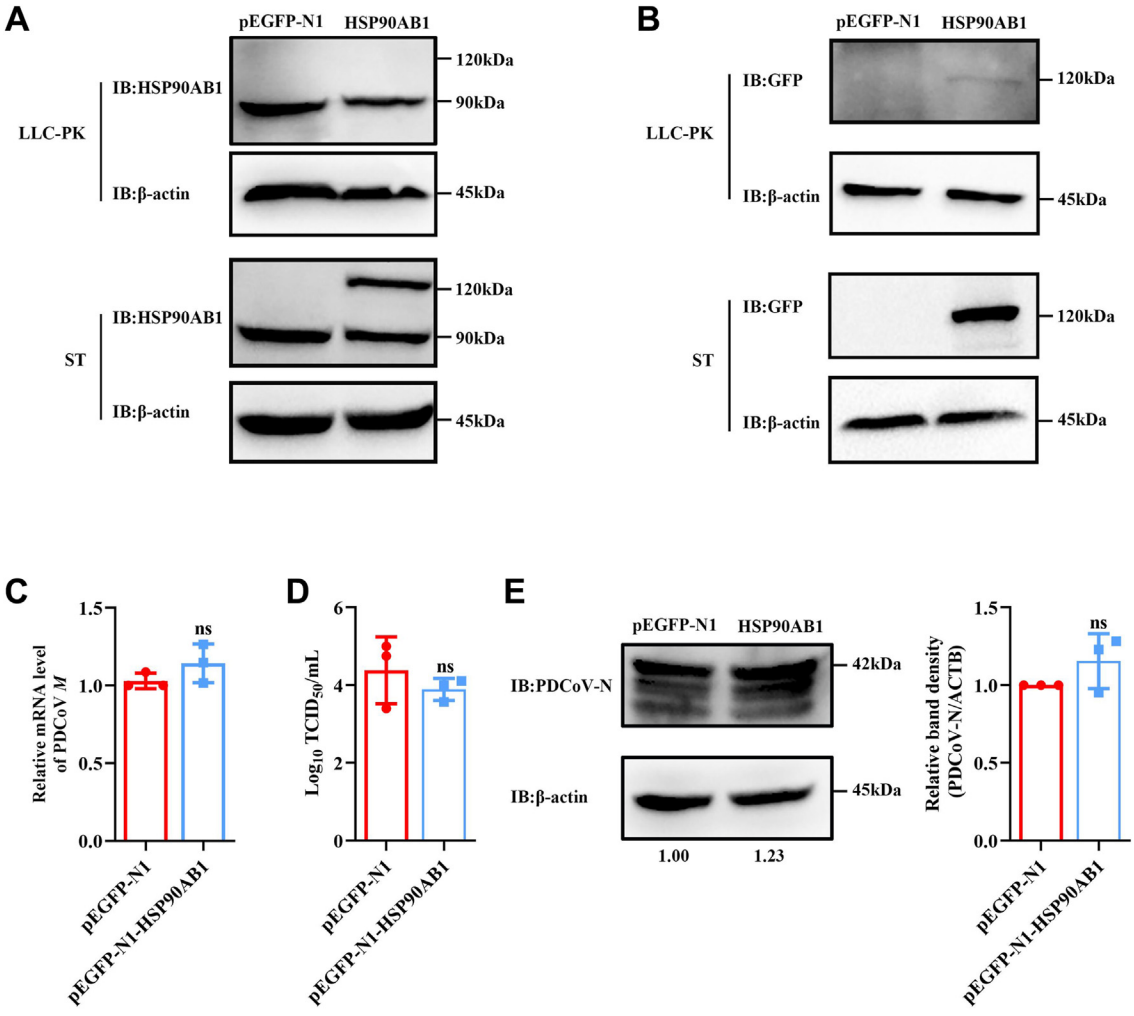

Figure 3. Overexpression of HSP90AB1 has no effect on PDCoV infection. *A* and *B*, overexpression of HSP90AB1 in the LLC-PK cells and ST cells was verified by Western blot using anti-HSP90AB1 antibody and anti-GFP antibody. *C*, qRT–PCR analysis of PDCoV *M* mRNA level in HSP90AB1-overexpressing ST cells. *D*, viral titer in the supernatant from PDCoV-infected HSP90AB1-overexpressing ST cells was detected by $TCID_{50}$. *E*, Western blot detection of PDCoV N protein expression in HSP90AB1-overexpressing ST cells. The band density of the protein was quantified using ImageJ software, and the PDCoV-N to ACTB ratios were normalized to the control. Data are shown as the mean ± SD from three independent experiments. HSP90AB1, heat shock protein 90 alpha family class B1; PDCoV, porcine deltacoronavirus; qRT–PCR, quantitative RT–PCR.

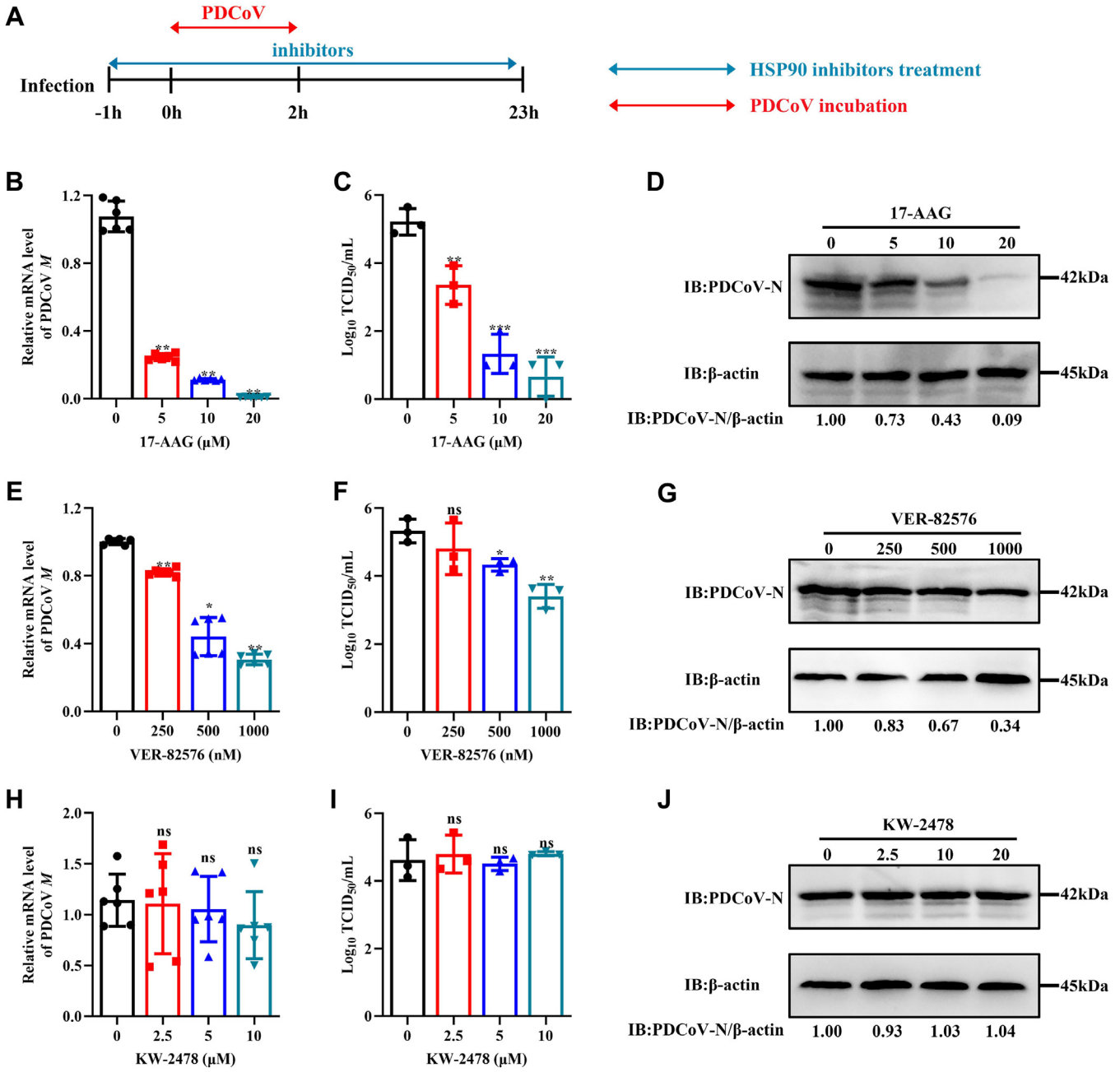

Figure 4. HSP90 ATPase activity is required for PDCoV infection. *A*, schematic of infection and inhibitor treatment time course. *Blue double-headed arrows* indicate the presence of HSP90 inhibitors, and *red double-headed arrows* indicate the incubation with PDCoV. PDCoV *M* mRNA levels in PDCoV-infected LLC-PK cells treated with (*B*) 17-AAG, (*E*) VER-82576, and (*H*) KW-2478. Viral titer in the supernatants from PDCoV-infected cells treated with (*C*) 17-AAG, (*F*) VER-82576, and (*I*) KW-2478. Western blots of PDCoV N protein from PDCoV-infected cells treated with (*D*) 17-AAG, (*G*) VER-82576, and (*J*) KW-2478. HSP90, heat shock protein 90; PDCoV, porcine deltacoronavirus.

KW-2478 (Fig. S3, *G* and *H*) had effect on *HSP90AA1* mRNA or protein levels. These results indicate that it is the ATPase activity of HSP90AB1 that is important in PDCoV infection.

PDCoV infection does not affect HSP90AB1 expression

To verify the influence of PDCoV infection on HSP90AB1 expression, LLC-PK cells were infected at a multiplicity of infection (MOI) of 0.1 and then harvested over a 24 h time course. qRT–PCR and Western blot results showed that PDCoV infection had no statistical effect on *HSP90AB1* mRNA or protein levels (Fig. S4).

HSP90AB1 affects the postentry stage of PDCoV infection

To determine which stages of the PDCoV life cycle are affected by HSP90AB1, we first evaluated viral entry in HSP90AB1^{KO} cells and WT cells treated with 17-AAG and VER-82576. Results showed that KO of *HSP90AB1* (Fig. S5, *A* and *D*), HSP90 inhibitors 17-AAG (Fig. S5, *B* and *E*) and VER-82576 (Fig. S5, *C* and *F*), had no significant effect on viral

adsorption and internalization, demonstrating that HSP90AB1 does not affect the entry stage of PDCoV infection.

To evaluate the effect of HSP90AB1 on viral postentry stage, LLC-PK cells were treated with 17-AAG or VER-82576 and infected with PDCoV. From samples taken at 3, 6, 12, and 18 hpi, qPCR, Western blot assays were done to quantitate viral *M* mRNA levels and N protein levels. The results showed that for both inhibitors, the greatest inhibition occurred at 12 hpi. At 3 hpi, there was no significant reduction in *M* gene levels over the mock-treated controls (Fig. 5, *A* and *F*). At 6 hpi, 5 μM 17-AAG and 250 nM VER-82576 treatment resulted in approximately 85% and 50% decrease in *M* mRNA levels, respectively (Fig. 5, *B* and *G*). At 12 and 18 hpi, *M* mRNA levels were just at the limit of detection in cells treated with 17-AAG (Fig. 5, *C* and *D*); in cells treated with 250 nM VER-82576, the decrease in *M* mRNA levels was about 80% and 50%, respectively (Fig. 5, *H* and *I*). The degree of reduction in N protein levels was similar (Fig. 5, *E* and *J*). These results suggest that HSP90AB1 affects PDCoV infection at the postentry stage and that 17-AAG is the more effective HSP90AB1 inhibitor.

HSP90AB1 interacts with multiple PDCoV proteins

Coimmunoprecipitation assays were performed to determine which viral proteins interact with HSP90AB1. Human embryonic kidney 293T (HEK293T) cells were cotransfected with pEGFP-N1-HSP90AB1 and pCMV-hemagglutinin (HA) expressing one of the viral proteins for 36 h. Whole-cell lysates were used to verify expression of the PDCoV proteins and HSP90AB1 (Figs. 6, *A–C*, S6, *A–C* and S7, *A–D*). Coimmunoprecipitations were performed using anti-GFP and anti-HA antibody. The HA-tagged viral proteins N, NSP10, and NS7 were detected in the immunoprecipitated complexes (Figs. 6,

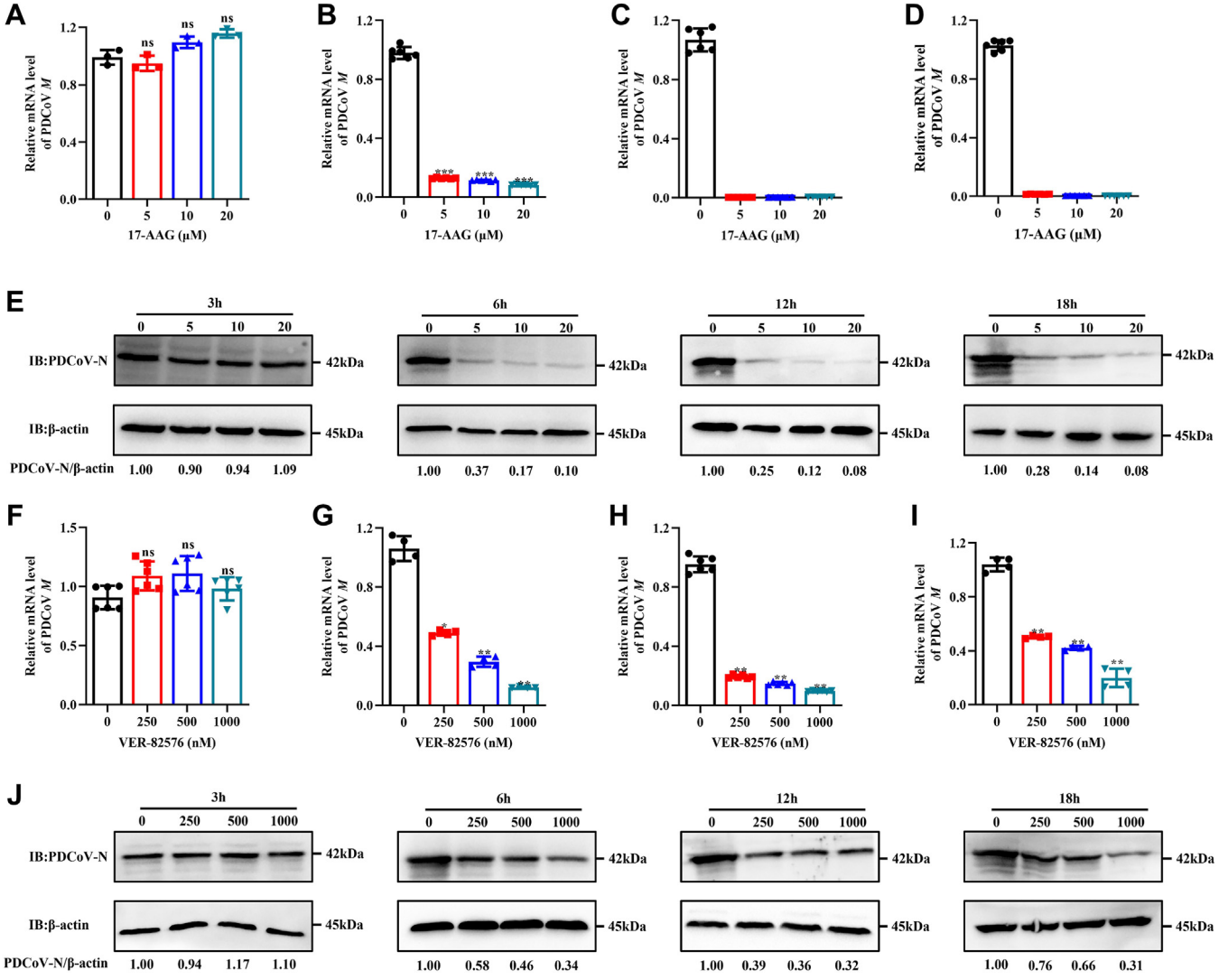

Figure 5. Inhibition of HSP90AB1 affects PDCoV infection at the postentry stage. *A–D*, qRT–PCR of PDCoV *M* mRNA from LLC-PK cells treated with 17-AAG and infected for 3, 6, 12, and 18 h, respectively. *E*, Western blot for the PDCoV N protein from the LLC-PK cells treated with 17-AAG. *F–I*, qRT–PCR of PDCoV *M* mRNA from LLC-PK cells treated with VER-82576 and infected for 3, 6, 12, and 18 h, respectively. *J*, Western blot for the PDCoV N protein from the LLC-PK cells treated with VER-82576. HSP90AB1, heat shock protein 90 alpha family class B1; PDCoV, porcine deltacoronavirus; qRT–PCR, quantitative RT–PCR.

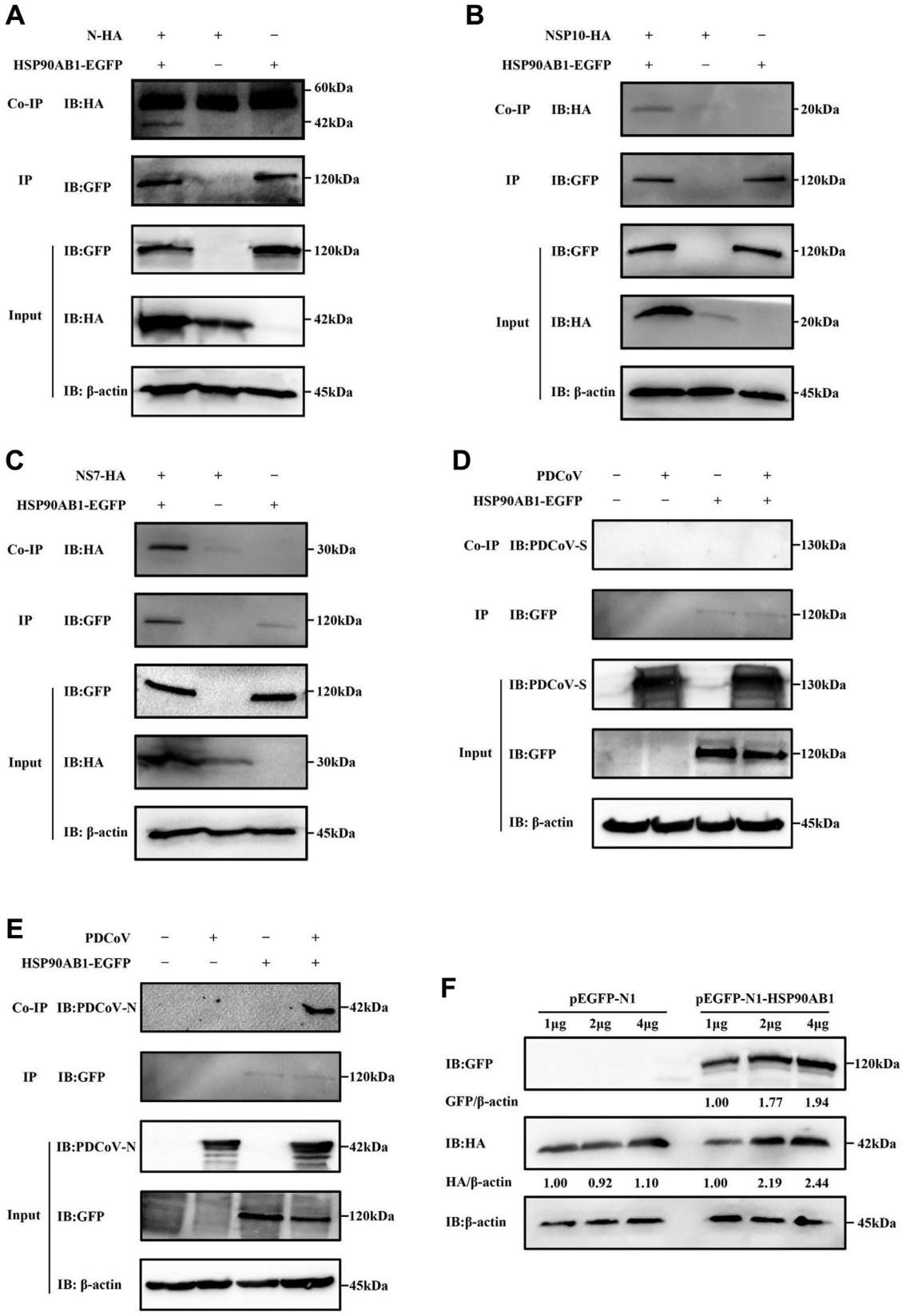

Figure 6. HSP90AB1 interacts with multiple PDCoV proteins. *A–C*, the interaction of HSP90AB1 and PDCoV proteins was identified using the co-IP assay. HEK293T cells were cotransfected with plasmids expressing GFP-tagged HSP90AB1 and (*A*) HA-tagged N, (*B*) NSP10, and (*C*) NS7 proteins. Whole-cell lysates were used for IP with anti-GFP antibody, the coprecipitated partner was detected by Western blot using an anti-HA antibody. *D* and *E*, ST cells overexpressing HSP90AB1 were infected with PDCoV and immunoprecipitated with anti-GFP antibody. Interactions between HSP90AB1 and (*D*) the viral S and (*E*) N proteins were analyzed. Coprecipitated partners in (*D* and *E*) are derived from the same immunoprecipitate, so IP IB:GFP in (*D* and *E*) is the same source image. *F*, HSP90AB1 regulates N protein expression in a dose-dependent manner. HEK293T cells were cotransfected with 1, 2, and 4 μg of plasmids expressing GFP-tagged HSP90AB1 and HA-tagged N. At 36 h post-transfection, Western blot was performed. co-IP, coimmunoprecipitation; HA, hemagglutinin; HEK293T, human embryonic kidney 293T cell line; HSP90AB1, heat shock protein 90 alpha family class B1; IB, immunoblotting; PDCoV, porcine deltacoronavirus.

A–*C* and S6, *A*–*C*). To rule out the potential influence of HSP90AB1 on coimmunoprecipitation signals, the protein loading volume was increased by a factor of five in cotransfected cells expressing pEGFP-N1-HSP90AB1 and pCMV-HA-N/NS7/NSP10 compared with those expressing pEGFP-N1 and pCMV-HA-N/NS7/NSP10. Western blot results showed that HA-tagged viral proteins N, NSP10, and NS7 were detected in the immunoprecipitated complexes, suggesting an interaction between HSP90AB1 and viral proteins N, NS7, or NSP10 (Fig. S6, *A*–*C*). ST cells were transfected with a GFP-tagged plasmid expressing HSP90AB1 protein and then infected with PDCoV for 24 h. Coimmunoprecipitations, performed using anti-GFP and anti-PDCoV S1-CTD (C-terminal domain) or anti-PDCoV N antibody, showed that HSP90AB1 coimmunoprecipitated with the viral N protein but not the S protein (Fig. 6, *D* and *E*). Moreover, we found that HSP90AB1 affects N protein expression in a dose-dependent manner (Fig. 6*F*). By confocal microscopy, we found that HSP90AB1 colocalizes with N, NS7, and NSP10 protein in the cytoplasm (Fig. 7). These results suggest that multiple PDCoV proteins can interact with HSP90AB1.

To determine which domain of the N protein interacts with HSP90AB1, plasmids expressing one of five N protein deletion mutants and pEGFP-N1-HSP90AB1 were cotransfected with HEK293T cells. Because the mutants N△NTD (N-terminal domain) and N△LKR (serine/arginine-rich linker region) were not expressed in the transfected cells (Fig. S8*A*), plasmids expressing HA-tagged NTD and LKR were constructed, and expression was verified by Western blot (Fig. S8*B*). Coimmunoprecipitation assay analysis showed that N△C-tail domain binds poorly to HSP90AB1 protein, compared with N protein (Fig. 8). Moreover, in the GFP pulldown to a level that was equal to NΔC-tail or N, the results showed that NΔCTD and NΔN-arm could be still detectable by Western blot (Fig. S8*C*). These results demonstrate that the C-tail domain of N protein is the potential domain interacting with HSP90AB1.

HSP90AB1 prevents PDCoV N protein degradation via *the proteasome pathway*

To examine whether the decrease of N protein expression level was related to the proteasome pathway or autophagy pathway, we utilized a specific proteasome inhibitor (MG-132) or autophagy inhibitor (chloroquine) during PDCoV infection. By CCK-8 assay, there was no detectable cytotoxicity from MG132 and chloroquine in LLC-PK cells at 250 nM and 80 μM, respectively (Fig. S2, *D* and *E*). Moreover, there was also no detectable cytotoxicity from 17-AAG, VER-82576, chloroquine, and MG132 in HEK293T cells at 1 μM, 1 μM, 10 μM, and 0.5 μM, respectively (Fig. S9). PDCoV-infected LLC-PK and uninfected HEK293T cells were transfected with pCMV-HA expressing N protein and treated with HSP90 inhibitors 17-AAG, VER-82576, MG132, chloroquine, 17-AAG combined with MG132 or chloroquine, and VER-

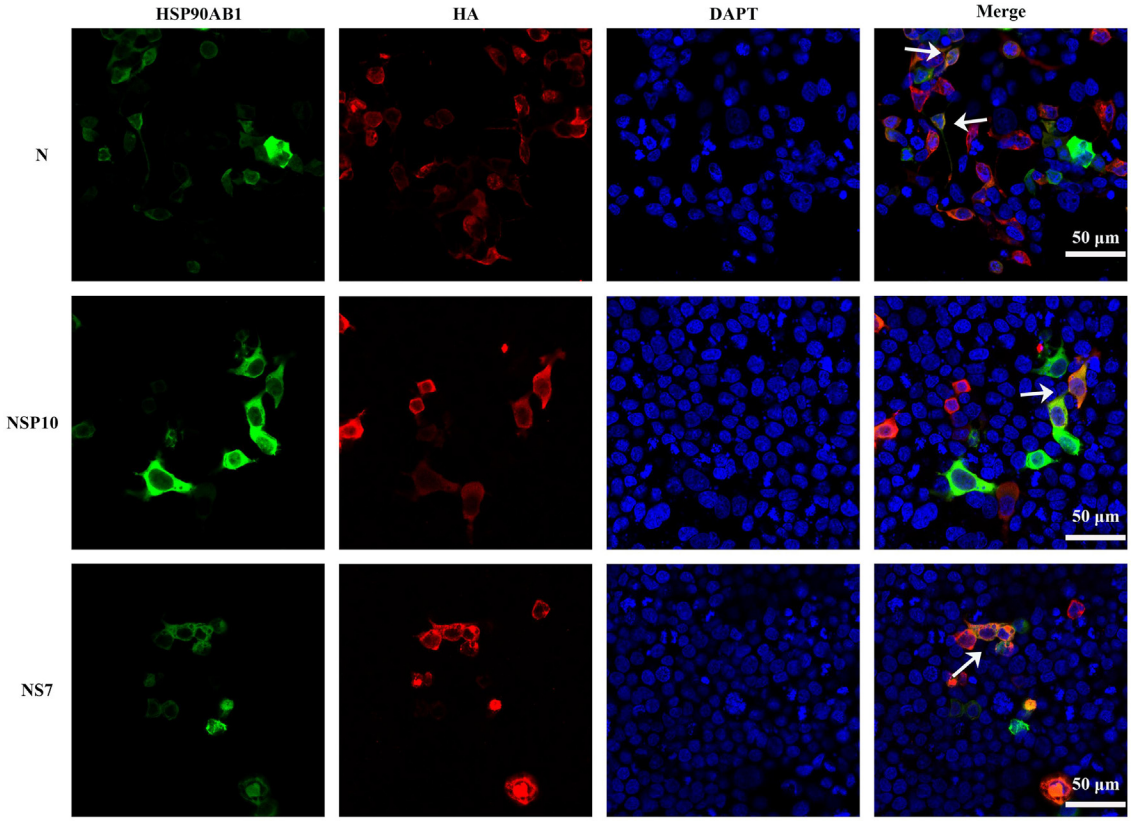

Figure 7. Colocalization of HSP90AB1 and PDCoV N, NS7, and NSP10 proteins. HEK293T cells were cotransfected with pEGFP-N1-HSP90AB1 and pCMV-HA-N, -NS7, or -NSP10. Cells were visualized by confocal microscopy. Magnification = 60×. HEK293T, human embryonic kidney 293T cell line; HSP90AB1, heat shock protein 90 alpha family class B1; PDCoV, porcine deltacoronavirus.

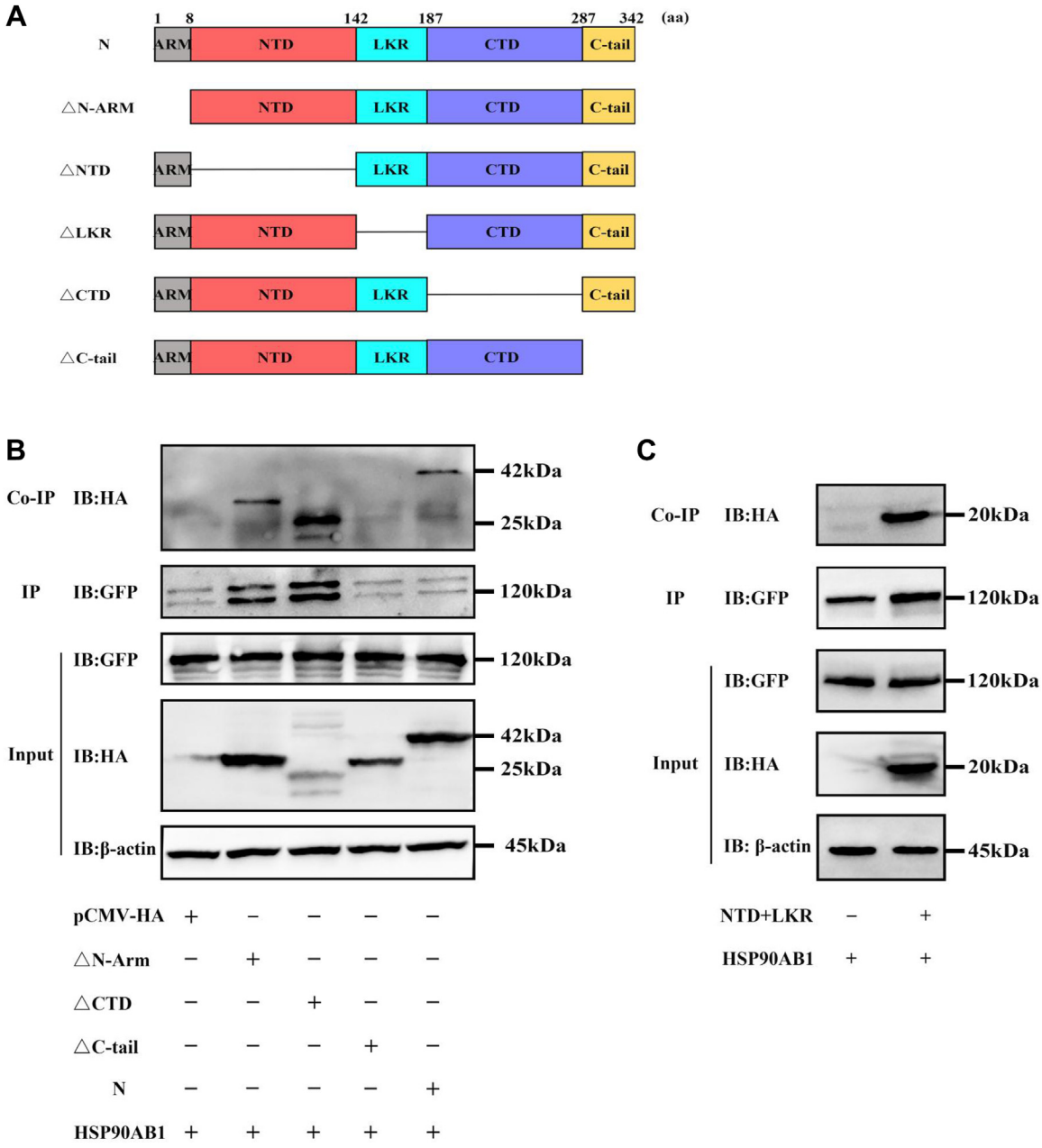

Figure 8. HSP90AB1 interacts with the C-tail domain of N protein. *A*, schematic diagram of PDCoV N protein and its truncated mutants. *B* and *C*, HEK293T cells were cotransfected with pEGFP-N1-HSP90AB1 together with (*B*) full-length N or its deletion mutants or with (*C*) NTD + LKR (its truncated mutant). The cell lysates were used for immunoprecipitation with an anti-GFP antibody, and the coprecipitated partner was detected by Western blot using an anti-HA antibody. HA, hemagglutinin; HEK293T, human embryonic kidney 293T cell line; HSP90AB1, heat shock protein 90 alpha family class B1; LKR, serine/arginine-rich linker region; NTD, N-terminal domain; PDCoV, porcine deltacoronavirus.

82576 combined with MG132 or chloroquine. Western blots showed that for all treatment combinations, except 17-AAG/MG-132 and VER-82576/MG-132, N protein levels were decreased over untreated infected cells. The N protein levels in the 17-AAG/MG-132 and VER-82576/MG-132 treated cells were near control levels (Fig. 9, *A* and *B*). These results show the decrease in N protein levels in HSP90AB1 KO or inhibited cells *via* the proteasome degradation pathway.

HSP90AB1^{WT} and HSP90AB1^{KO} cells were infected with PDCoV; at 12 hpi, cells were treated with MG132 or chloroquine and incubated for a further 12 h. Cell lysates were analyzed by Western blot. As shown in Figure 9*C*, in infected HSP90AB1^{KO} cells (not treated with inhibitor), N protein levels were 51% less than in WT cells. In infected WT cells treated with MG132 or chloroquine, N protein levels were 42% and 30% less respectively than in untreated WT cells. In infected HSP90AB1^{KO} cells treated with MG132, the N protein levels were near WT levels, whereas in infected HSP90AB1^{KO} cells treated with chloroquine, they were less than in chloroquine-treated WT cells.

In addition, in HSP90AB1^{WT} and KO cells, mRNA levels of E3 ubiquitin ligase, including *CHIP* (carboxyl terminus of the

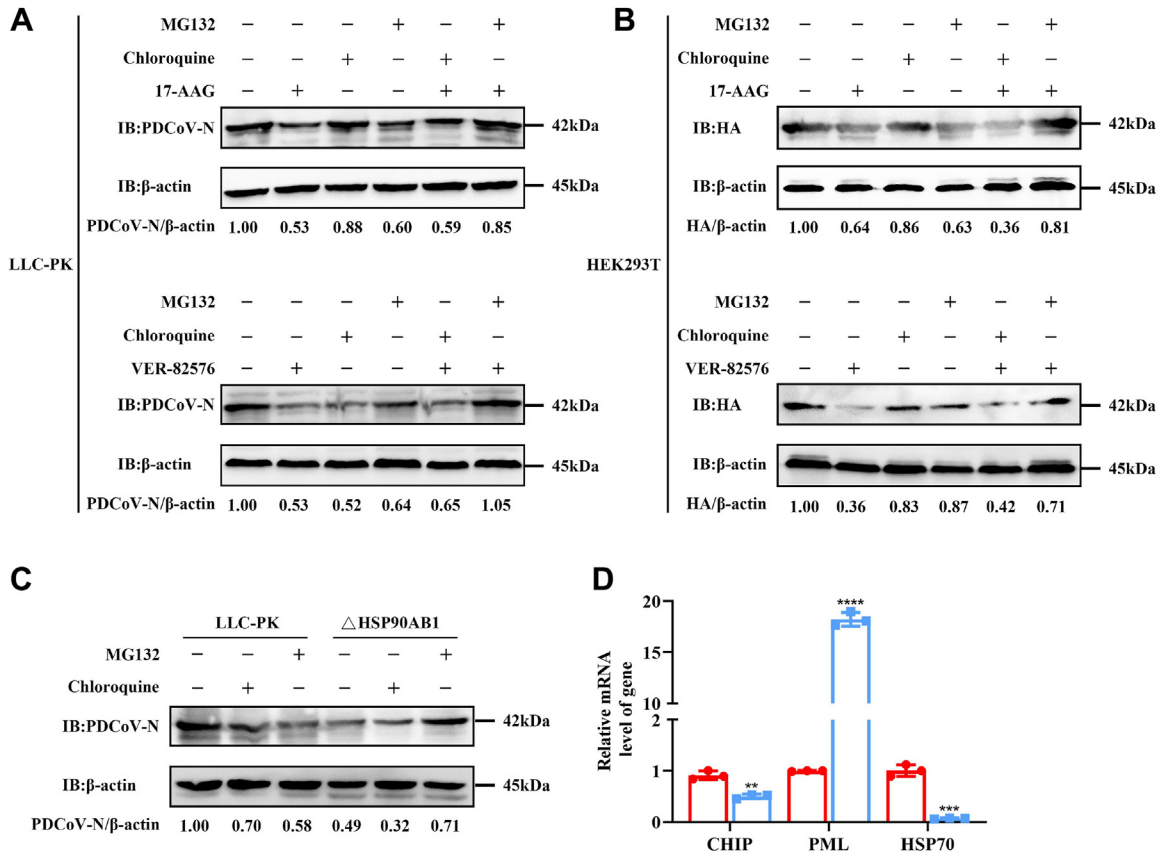

Figure 9. HSP90AB1 protects PDCoV N protein from degradation *via* the proteasome pathway. Western blots for N protein from (*A*) LLC-PK infected with PDCoV and (*B*) HEK293T cells transfected with pCMV-HA-N treated separately with MG132, chloroquine, 17-AAG, and VER-82576, and the combinations of 17-AAG or VER-82576 along with MG132 or chloroquine. *C*, WT and KO cells were infected with PDCoV and treated with MG132 or chloroquine at 12 hpi. Cell lysates were analyzed by Western blot. *D*, the *CHIP*, *PML*, and *HSP70* mRNA levels were quantitated by qRT–PCR. The band density of the protein was quantified using ImageJ software, and the PDCoV-N to ACTB ratios were normalized to the control. Data are shown as the mean ± SD from three independent experiments. HEK293T, human embryonic kidney 293T cell line; HSP90AB1, heat shock protein 90 alpha family class B1; PDCoV, porcine deltacoronavirus; qRT–PCR, quantitative RT–PCR.

HSP70-interacting protein), *PML* (promyelocytic leukemia), and HSP90 cochaperone *HSP70*, were quantified by qRT–PCR. As shown in Figure 9*D*, HSP90AB1 KO resulted in a 52% and 94% decrease of *CHIP* and *HSP70* mRNA levels, respectively, and an 18-fold increase in *PML* mRNA, indicating that the decrease of N protein expression resulted by HSP90AB1 KO is associated with ubiquitin-mediated proteasome degradation.

Discussion

Viruses rely on the host cellular machinery to complete their life cycles, and some host factors play pivotal roles in viral infection. Based on traditional methods, the role of some host factors (pAPN (33), cholesterol 25-hydroxylase (17), signal transducer and activator of transcription 1 (18), and TMEM41B (19)) in PDCoV infection have been identified. Here, using genome-wide CRISPR screening, we identified HSP90AB1 as a host factor that enhances PDCoV infection and elucidate the mechanism by which it does so.

CRISPR genome-wide screening has been used to identify host factors involved in viral infection, such as TMEM41B contribution to TGEV internalization and early stage replication (19), zinc finger DHHC-type palmitoyltransferase 17 for SADS-CoV genomic RNA replication (26), and placenta-associated eight for SADS-CoV subgenomic RNA expression (27). Here, we used CRISPR genome-wide screening to identify host factors in LLC-PK cells that play a role in PDCoV infection. Our analysis revealed that sgRNAs targeting *CPSF2*, *HSP90AB1*, *SLC27A4*, *CCDC124*, *TOMM6*, *EDIL3*, *SLC9A5*, and *DCTN1* were the most enriched candidate genes. Using MAGeCK algorithm method, *HSP90AB1* was the most enriched host factor (Fig. 1) and was therefore chosen for further study.

HSP90AB1, a highly conserved molecular chaperone, has been shown to be beneficial for human coronavirus infection. For example, HSP90AB1 is involved in MERS-CoV infection and helps stabilize the viral N protein (29); it also regulates SARS-CoV-2 infection *via* binding viral RNA (31). Inhibition of HSP90 by 17-AAG significantly reduced SARS-CoV and SARS-CoV-2 infection (29). Transcriptomic analysis identified HSP90AA1 as a host factor relevant for SARS-CoV-2 infection in human cell lines (32). PDCoV replication in HSP90AB1^{KD} or HSP90AB1^{KO} cells was significantly less than in WT cells (Figs. S1 and 2), indicating that HSP90AB1 is a host factor beneficial to PDCoV infection. HSP90 inhibitors are small

molecules that compete with ATP for HSP90 binding, thereby suppressing its ATPase activity (34). In PDCoV-infected cells, treatment with HSP90AB1 inhibitors 17-AAG and VER-82576 resulted in significantly reduced PDCoV titers (Fig. 4). The inhibitors did not however affect HSP90AB1 expression levels or viral attachment and internalization (Figs. S3 and S5). These results indicated that HSP90AB1 ATPase activity is what is enhancing PDCoV infection. KD of HSP90AB1 resulted in the greatest reduction of PDCoV levels at 6 hpi (Fig. S1), and the greatest inhibitory effect of 17-AAG and VER-82576 occurred at 12 hpi (Fig. 5), whereas HSP90AB1 had no effect on PDCoV infection at 3 hpi (Figs. S1 and 5), suggesting that the effect of HSP90AB1 on PDCoV infection occurs at the postentry stage. Moreover, our study also showed that HSP90AB1 was a critical host factor for TGEV and porcine epidemic diarrhea virus infection (unpublished data), indicating HSP90AB1 can function as a common candidate therapeutic target in porcine diarrhea diseases.

Some viruses induce overexpression of HSPs in infected cells (35). For example, HSPA1B (a member of the HSP70 protein family) as well as mitochondrial 60 kDa HSP (HSP60) are both upregulated in TGEV-infected ST cells (36). Several HSPs are associated with some viral infection, for example, HSP90 and HSP70 are components of dengue virus receptor complex, mediating viral entry into human cells (37); they can also synergistically increase hepatitis B virus capsid assembly (38). Here, we found that PDCoV infection had no effect on HSP90AB1 expression at any postinfection time point tested (Fig. S4). These results are consistent with Ma *et al.* (36) who found that HSP90α and HSP90β were unchanged at 48 hpi in TGEV-infected ST cells. Interestingly, expression of these two proteins was significantly downregulated at 64 hpi, indicating that viral infection time might have an influence on the expression of HSPs.

Viral proteins, such as p150 of rubella virus (39), VP5 protein of pseudorabies virus (40), neuraminidase protein of influenza A virus (41), and N protein of MERS-CoV (29), are HSP90 client proteins, and HSP90 is required for maintaining their stability. Moreover, the interaction of HSP90 and client proteins can facilitate viral infection by regulating various cellular signaling pathways (42, 43). HSP90 can also regulate client protein expression level (30). Using coexpression and coimmunoprecipitation assays, we found that HSP90AB1 affects N protein expression in a dose-dependent manner and interacts with PDCoV proteins N, NS7, and NSP10 (Figs. 6 and 7). However, coimmunoprecipitation signals can be solely attributed to elevated expression resulting from HSP90AB1-enhanced viral protein level. To rule out this possibility, we conducted this assay by adjusting the volume of the loading samples and found that HA-tagged viral proteins N, NSP10, and NS7 were detected in the immunoprecipitated complexes. These findings indicated that HSP90AB1 could interact with N, NS7, and NSP10 (Fig. S6). With further investigation, we found that HSP90AB-interaction domain of the N protein is its C-tail domain (Fig. 8), indicating that N, NS7, and NSP10 proteins might function as HSP90AB1 client proteins. However, NTD + LKR and other mutant constructs were obtained from distinct polyvinylidene difluoride membranes, and the GFP pulldown level of NTD + LKR was not subjected to adjust. Therefore, interaction of NTD + LKR domain of N protein and HSP90AB1 remained inconclusive.

The N protein is the main PDCoV structural protein and plays a critical role in viral assembly (44). In addition, it also promotes viral transcription and replication and modulates the processes of inflammatory cytokine production and apoptosis (45). Proteomic analyses have shown that PDCoV N protein upregulates expression of *HSP70* (heat shock cognate protein 70) and *GRP78* (glucose-regulated protein 78) (46), whereas NS7 downregulates *ACTN4* and *CPS1* (carbamoyl phosphate synthase 1) (47). N and NSP10 proteins can act as interferon antagonists, counteracting the host innate immune defense (48, 49). Of these three PDCoV proteins that interact with HSP90AB1, N protein has been reported to be involved in regulating the expression of HSPs (46), and our results demonstrate that HSP90AB1 affects N protein expression in a dose-dependent manner (Fig. 6*F*). Therefore, we chose PDCoV N protein for further analysis.

In addition to protein kinases and transcription factors, numerous viral proteins are identified as HSP90 client proteins, which can be degraded *via* the proteasome or autophagy pathway (39, 41, 50). Considering this, we utilized a specific proteasome inhibitor, MG-132, and autophagy inhibitor, chloroquine, to evaluate whether the decrease in N protein levels in infected KO cells and HSP90AB1-inhibited cells was the result of protein degradation through one of these pathways. The results indicated that HSP90AB1 protects N protein from degradation *via* the proteasome pathway (Fig. 9). E3 ubiquitin ligase CHIP can mediate the ubiquitination and degradation of chaperone-bound proteins *via* interaction with HSP70 or HSP90 (51). In addition, inhibition of HSP70 activity potentiates proteasome-dependent degradation of HSP90 client proteins (52). In this study, HSP90AB1 KO resulted in significantly decreased levels of *CHIP* and *HSP70* mRNA levels, particularly *HSP70* that was reduced by approximately 94% (Fig. 9*D*), indicating that HSP90AB1 and HSP70 might synergistically mediate PDCoV infection. PML, also called TRIM19, is a member of the tripartite motif (TRIM) family, which can positively regulate innate immune signaling pathways by acting as E3-Ub ligases (53). Our results showed that HSP90AB1 KO resulted in an 18-fold increase in *PML* mRNA levels (Fig. 9*D*), indicating that the reduction in N protein levels resulting from HSP90AB1 KO or inhibition might be associated with PML-mediated proteasome degradation pathway or PML-mediated innate immune signaling pathways; further studies are needed to verify this phenomenon.

To our knowledge, this is the first identification of HSP90AB1 as a host factor for PDCoV replication, and that it is HSP90AB1's ATPase activity that positively affects viral replication. HSP90AB1 interacts with PDCoV N, NS7, and NSP10 proteins and prevents degradation of N *via* the proteasome pathway. Our findings provide new insight into the mechanisms of PDCoV–host interactions and contribute to providing new host targets for PDCoV antiviral research.

Experimental procedures

Cells, virus, inhibitors, and antibodies

LLC-PK, ST, and HEK293T cells were maintained in Dulbecco's modified Eagle's medium (DMEM) (Gibco) supplemented with 10% fetal bovine serum (PNA) and 1% antibiotic–antimycotic (Solarbio) and incubated in a humidified atmosphere of 5% CO_2 at 37 °C. PDCoV strain CHN-SC2015 (GenBank accession no.: MK355396) was isolated in Sichuan province in 2018 (3). HSP90 inhibitor 17-AAG (CAS no.: 75747-14-7), proteasome inhibitor MG-132 (CAS no.: 1211877-36-9), and autophagy inhibitor chloroquine (CAS no.: 54-05-7) were purchased from Selleck Chemicals. HSP90 inhibitors KW-2478 (CAS no.: 819812-04-9) and VER-82576 (CAS no.: 847559-80-2) were purchased from MedChemExpress. Anti-HSP90AB1 rabbit polyclonal antibody (11405-1-AP), anti-HSP90AA1 rabbit polyclonal antibody (13171-1-AP), anti-GFP tag rabbit polyclonal antibody (50430-2-AP), and anti-HA tag rabbit polyclonal antibody (51064-2-AP) were purchased from Proteintech Group. Anti-PDCoV N and S1-CTD mouse monoclonal antibodies were prepared by our laboratory (54). Horseradish peroxidase (HRP)–conjugated goat antimouse immunoglobulin G (IgG) (AS003), HRP-conjugated goat anti-rabbit IgG (AS014), anti-GFP tag mouse monoclonal antibody (AE012), anti-HA tag mouse monoclonal antibody (AE008), and anti-ACTB rabbit polyclonal antibody (AC026) were purchased from ABclonal. Alexa Fluor 555-labeled donkey antimouse IgG (A0460) was purchased from Beyotime Biotechnology.

Cell culture, plasmids, and transfection

The coding sequence of porcine HSP90AB1 was synthesized by Sangon Biotech and ligated into a pEGFP-N1 expression vector with NheI and KpnI. The sequences for viral proteins E, M, N, NS6, NS7, NSP5, NSP10, and NSP15 were amplified from viral complementary DNA and ligated into a pCMV-HA expression vector with EcoRI and XhoI. N protein deletion mutants: NΔARM, NΔNTD, NΔLKR (linker domain) NΔCTD, and NΔC-tail domain and the coding sequences of NTD + LKR domain were ligated into pCMV-HA with EcoRI and XhoI. Primers are listed in Table 1. All recombinant plasmids were constructed by homologous recombination using a 2× Seamless Cloning Mix (Biomed) and were verified by sequencing. And then, pEGFP-N1-HSP90AB1 was transfected into LLC-PK cells or ST cells to generate a cell line with exogenous expression of HSP90AB1 protein. The remaining constructed plasmids were transfected into HEK293T cells for subsequent coimmunoprecipitation assay.

Generation of GeCKO library cells and PDCoV infection

LLC-PK cells at 50% confluence in T25 flasks were transduced with a designated LLC-PK-Cas9. After blasticidin (Solarbio) selection, cells were infected with lentiviruses encoding a pig CRISPR KO pooled sgRNA library at a MOI of 0.3. At 2 days post-transduction, 4 μg/ml puromycin (Solarbio) was added to the transduced LLC-PK-Cas9 cells; cells were maintained in selection media for 7 days. Cells were then incubated with 0.04 MOI PDCoV for 3 days and then washed with PBS and incubated in fresh medium with 10% fetal bovine serum. PDCoV-resistant cells were harvested and expanded to isolate genomic DNA for Illumina sequencing.

Generation of HSP90AB1 KO cells using the CRISPR–Cas9 system

An sgRNA targeting exon 7 was synthesized and inserted into a lentiCRISPR v2 vector (Addgene plasmid 52961) to generate a

Table 1
Primers used for PDCoV genes

Target	Primer sequences (5′-3′)
N	F: tggccatggaggccc**gaatt**GCCACCATGGCTGCACCAGTGGTCCCTACTA
	R: ccgcggccgcggtac**ctcgag**CTACGCTGCTGATTCCTGCTTTAT
M	F: tggccatggaggccc**gaatt**GCCACCATGTCTGACGCAGAAGAGTGG
	R: ccgcggccgcggtac**ctcgag**TTACATATACTTATACAGGCGAGCG
E	F: tggccatggaggccc**gaatt**GCCACCATGGTAGTCGACGACTGGGC
	R: ccgcggccgcggtac**ctcgag**TCAGACATAGTGAGTGTTTCTAGGA
NSP5	F: tggccatggaggccc**gaatt**GCCACCGCAGGTATCAAAATCCTCCTGC
	R: ccgcggccgcggtac**ctcgag**CTGCAATGAAATTGGAGCCTGA
NSP10	F: tggccatggaggccc**gaatt**GCCACCGCAAGTGGCACTCAAATTGAGTAC
	R: ccgcggccgcggtac**ctcgag**ACTAGATCCACAGGTGCAGTCATAA
NSP15	F: tggccatggaggccc**gaatt**GCCACCAACCTTGAAAACTTAGCTTACAACTG
	R: ccgcggccgcggtac**ctcgag**CTGTAAGATTGGGTAGCAAGTCTTG
NS6	F: tggccatggaggccc**gaatt**GCCACCATGTGCAACTGCCATCTGCA
	R: ccgcggccgcggtac**ctcgag**TTAATTTAATTCATCTTCAAGAATG
NS7	F: tggccatggaggccc**gaatt**GCCACCGAGTTCCGCTTAACTCCGC
	R: ccgcggccgcggtac**ctcgag**CTAGAGCCATGATGCGAGGAT
ΔN-ARM	F: tggccatggaggccc**gaatt**GCCACCACTGACGCGTCTTGGTTTCAGG
	R: ccgcggccgcggtac**ctcgag**CGCTGCTGATTCCTGCTTTATCTC
N-ARM + NTD	F: tggccatggaggccc**gaatt**GCCACCATGGCTGCACCAGTGGTCC
	R: cttgGGGGTCAACTCTGAAACCTTGA
CTD + C-Tail	F: tttcagagttgaccccCAAGCTCCCAAGCGGACTT
	R: ccgcggccgcggtac**ctcgag**CGCTGCTGATTCCTGCTTTAT
ΔC-tail	F: tggccatggaggccc**gaatt**GCCACCATGGCTGCACCAGTGGTCC
	R: ccgcggccgcggtac**ctcgag**CTGGTTAACGACCGTATTGAGCG
*NTD + LK*R	F: ggccatggaggccc**gaatt**ACTGACGCGTCTTGGTTTCAG
	R: ccgcggccgcggtac**ctcgag**ATGTTGGGTCTTACGACGTACC

Homologous arms are represented by lowercase letters; Restriction sites are represented by bold lowercase letters.

deletion or/and insertion mutation within *HSP90AB1* in LLC-PK cells. The sgRNA sequences were as follows: sgRNA-F, CACC-GAGGTCAAAAGGAGCCCGACG and sgRNA-R, AAACC GTCGGGCTCCTTTTGACCTC. The sgRNA expression plasmid was packaged into lentivirus particles in HEK293T cells by cotransfection with psPAX2 (Addgene plasmid 12260) and pMD2.G (Addgene plasmid 12259) at a ratio of 5:3:2. 48 h after transfection, and supernatants were collected and centrifuged 5000 rpm for 10 min at 4 °C. Lentiviruses were then transduced into LLC-PK cells that were approximately 50% confluent. After infection for 36 h, cells were subjected to selection with 4 μg/ml puromycin for 7 days. Genomic DNA was extracted from puromycin-resistant LLC-PK cells using a TIANamp Genomic DNA Kit (TianGen). *HSP90AB1* was detected in the purified genomic DNA by PCR amplification with primers that annealed approximately 250 bp upstream and downstream. The primer sequences were as follows: F, TGGATTTCTCTCACAGC ACTTC and R, TTCCTTTGAGAAAGCTGAGACC. The PCR products were sequenced by Sangon Biotech. *HSP90AB1* KO clonal cell lines (designated HSP90AB1^{KO}) were isolated by dilution and identified using qRT–PCR and Western blot.

Cell viability assay

The cytotoxicity of inhibitors was assessed using a CCK-8 (Meilun). Briefly, 100 μl of 10^5 LLC-PK or HEK293T cells/ml were aliquoted into wells of 96-well plates and incubated for 24 h. Cells were then treated with a series of inhibitor concentrations in serum-free DMEM for 24 h. Mock-treated cells and DMEM without inhibitor served as the negative control and blank control, respectively. After washing with PBS, cells were incubated for 1 h at 37 °C with 10 μl CCK-8 reagent per well. Absorbance was measured at 450 nm using a microplate reader (Thermo Scientific). Cytotoxicity was calculated as ([mean absorbance at 450 nm inhibitor-mean absorbance at 450 nm blank]/[mean absorbance at 450 nm control-mean absorbance at 450 nm blank]) × 100%.

HSP90 inhibition

LC-PK cells were treated with 17-AAG (0, 5, 10, and 20 μM), VER-82576 (0, 250, 500, and 1000 nM), and KW-2478 (0, 5, 10, and 20 μM) for 1 h and then infected with PDCoV in the presence of inhibitors and incubated for 2 h at 37 °C. The virus-drug overlay was removed, and cells were cultured with maintenance medium containing inhibitors for another 21 h. PDCoV *M* mRNA levels and N protein levels were detected by qRT–PCR and Western blot, respectively.

Viral attachment and internalization assays

For the viral attachment assays, LLC-PK cells treated with HSP90 inhibitors, 17-AAG and VER-82576, or HSP90AB1^{WT} and HSP90AB1^{KO} cells were incubated with PDCoV (MOI = 10) for 1 h at 4 °C. Unattached virus was removed by washing three times with cold PBS. Cells were then collected to quantify the amount of bound virus, and the level of PDCoV *M* mRNA was determined by qRT–PCR. For the viral internalization assay, cells were incubated with PDCoV (MOI = 10) for 1 h at 4 °C to allow for viral attachment. Infected cells were washed three times with cold PBS and incubated at 37 °C for another 1 h to allow for viral internalization. Cells were then washed three times with cold citrate buffer (pH = 3) (Solarbio) to remove the bound, but noninternalized, viral particles. The cells were collected, and the level of PDCoV *M* mRNA was determined by qRT–PCR.

Coimmunoprecipitation assay

A pEGFP-N1 plasmid expressing HSP90AB1 and HA-tagged plasmids expressing PDCoV proteins were constructed. PDCoV proteins include structural proteins, envelope (E), membrane (M), and N, two accessory proteins (NS6 and NS7), and three nonstructural proteins (NSP5, NSP10, and NSP15). HEK293T cells at 50% confluence in 6-well plates were cotransfected with pEGFP-N1-HSP90AB1 and one of the HA-tagged plasmids or blank vector using Lipofectamine 3000 (Sigma–Aldrich). At 36 h post-transfection, coimmunoprecipitation assays were performed using SureBeads protein G magnetic beads (Bio-Rad). Briefly, the magnetic beads were washed three times and incubated with anti-GFP antibody (1:100 dilution) at 4 °C for 8 h. After washing, beads were incubated with 100 μl of PDCoV protein overnight at 4 °C. Beads were collected, washed, and then incubated with 50 μl of 1× protein loading buffer in a boiling water bath for 5 min. The eluents were used for Western blot analysis.

Immunofluorescence staining

HEK293T cells were cotransfected with pEGFP-N1-HSP90AB1 and the HA-tagged plasmids expressing N, NS7, or NSP10. At 36 h post-transfection, the cells were fixed with 4% paraformaldehyde for 30 min at room temperature. Cells were rinsed with PBS and permeabilized with 0.5% Triton-X-100 in PBS for 30 min at room temperature. Cells were rinsed three times with PBS for 5 min per rinse and then blocked with 2% bovine serum albumin in PBS for 1 h at 37 °C. Cells were incubated for overnight at 4 °C with anti-HA tag mouse monoclonal antibody diluted 1:200 in 2% bovine serum albumin. Cells were washed again and then incubated with Alexa Fluor 555-labeled donkey antimouse IgG secondary antibody (1:200 dilution in PBS with Tween-20) for 1 h at room temperature, followed by treatment with 4′,6-diamidino-2-phenylindole for 10 min to stain nuclei. Confocal images were acquired using a NIKON Eclipse Ti.

qRT–PCR

Total RNA was extracted from PDCoV-infected cells using a UNIQ-10 column TRIzol total RNA Isolation Kit (Sangon). RNA was reverse transcribed using a PrimeScript RT Reagent Kit with gDNA Eraser (Takara). The complementary DNA was used for qRT–PCR with TB Green Premix Ex Taq II (primers shown in Table 2). Relative mRNA levels were calculated using the $2^{-\Delta\Delta CT}$ method with *ACTB* used as an internal control. qRT–PCR was performed on a LightCycler 96 system (Roche) using the following conditions: 95 °C for 30 s, then 40 cycles of 95 °C for 5 s, 55 °C for 30 s, and 72 °C for 30 s. Each

Table 2
Primers used for qRT–PCR

Gene	Sequence (5′-3′)	Size (bp)
PDCoV M	F: CCAATGGGTACATGGAGGT R: GTGGCGGATTTCTAACTGA	130
HSP90AB1	F: TGGAGAGTTCTACAAAAGCCTG R: CTTCAAAATCTTGCTCTGCTG	304
HSP90AA1	F: CTTCCTCTGAACATTTCTCGTG R: GATGTGTTTCTGGTTCTCCTTC	294
HSP70	F: GCACGAGGAAAGCCTTAGAG R: GGAGAAGATGGGACGACAAA	166
PML	F: GCACCTCTAAGGCAGTCTCAC R: TGGCTTTCTTGGTTCACGG	373
CHIP	F: ACCACGAGGGTGAAGAGGAT R: TCCGAGTCACAGGGTCAAAG	270
Porcine *ACTB*	F: CTTCCTGGGCATGGAGTCC R: GGCGCGATGATCTTGATCTTC	201

experiment consisted of three biological replicates, and the qRT–PCR for each sample was done in triplicate.

Western blot

Cells were washed twice with cold PBS and then incubated for 15 min at 4 °C in radioimmunoprecipitation assay lysis buffer with PMSF (Solarbio). Lysates were centrifugated at 12,000 rpm for 5 min at 4 °C, and the supernatants were collected. About 10 μl of supernatants were subjected to SDS-PAGE and then transferred to polyvinylidene difluoride membrane (Bio-Rad) for 60 min at 250 mA. Membranes were blocked for 2 h at room temperature with 5% (w/v) skim milk in Tris-buffered saline with Tween-20 (0.05% Tween-20, 0.15 M NaCl, 1 mM Tris–HCl, pH 7.5) and then incubated overnight with either mouse monoclonal antibodies, PDCoV N (1:500), PDCoV S1-CTD (1:500), GFP (1:1000), or rabbit polyclonal antibodies, ACTB (1:10,000), HA (1:1000), PDCoV N (1:200), HSP90AB1 (1:1000), and HSP90AA1 (1:1000). All antibodies were diluted in Primary Antibody Dilution Buffer (Beyotime). Membranes were washed four times for 4 min with Tris-buffered saline with Tween-20 and then incubated for 45 min at room temperature with 1:5000 HRP-conjugated goat anti-mouse or anti-rabbit IgG. Membranes were washed again, and protein bands were visualized by addition of ECL (Bio-Rad) according to the manufacturer's instructions and quantified using ImageJ software (National Institute of Health).

$TCID_{50}$

Confluent cell monolayers seeded in 96-well plates were washed twice with maintenance medium and then inoculated with 100 μl of 10-fold serially diluted PDCoV. At each dilution, there were eight technical replicates. About 150 μl of maintenance medium was added to each well after the cells and virus had incubated for 1.5 h at 37 °C. The cytopathic effect was observed for 4 days and analyzed by the methods of Reed and Muench (55).

Statistical analysis

All experiments were performed in triplicate. Data are shown as the mean ± SD. Student's *t* test was used to measure significant differences between two groups. p Values <0.05 were considered statistically significant.

Data availability

All data generated or analyzed during this study are included in this published article.

Supporting information—This article contains supporting information.

Acknowledgments—This study was supported by the National Natural Science Foundation of China (grant no.: 32172888), the Sichuan Science and Technology Program (grant no.: 2021ZDZX0010), and the Major Science and Technology Project of Yunnan Province (grant no.: 202102AE090039).

Author contributions—S. C. and Xiaobo Huang conceptualization; Y. W., R. W., Q. Z., S. D., Q. Y., Xinfeng Han, and X. W. formal analysis; Y. Z., J. Y., D. X., L. Z., C. L., J. H., R. C., and D. S. investigation; S. C. and Xiaobo Huang resources; Y. Z. writing–original draft; Xiaobo Huang writing–review & editing; Xiaobo Huang funding acquisition.

Conflict of interest—The authors declare that they have no conflicts of interest with the contents of this article.

Abbreviations—The abbreviations used are: APN, aminopeptidase N; CCK-8, Cell Counting Kit-8; CHIP, carboxyl terminus of the HSP70-interacting protein; CTD, C-terminal domain; DMEM, Dulbecco's modified Eagle's medium; HA, hemagglutinin; HEK293T, human embryonic kidney 293T cell line; HRP, horseradish peroxidase; HSP, heat shock protein; HSP90AB1, heat shock protein 90 alpha family class B1; IgG, immunoglobulin G; KD, knockdown; LKR, serine/arginine-rich linker region; MERS-CoV, middle east respiratory syndrome coronavirus; MOI, multiplicity of infection; NTD, N-terminal domain; PDCoV, porcine deltacoronavirus; PML, promyelocytic leukemia; qRT–PCR, quantitative RT–PCR; SADS-CoV, swine acute diarrhea syndrome coronavirus; SARS-CoV-2, severe acute respiratory syndrome coronavirus 2; sgRNA, single-guide RNAs; TGEV, transmissible gastroenteritis virus; TMEM41B, transmembrane protein 41B.

References

1. Jung, K., Hu, H., and Saif, L. J. (2016) Porcine deltacoronavirus infection: etiology, cell culture for virus isolation and propagation, molecular epidemiology and pathogenesis. *Virus Res.* **226**, 50–59
2. Le, V. P., Song, S., An, B. H., Park, G. N., Pham, N. T., Le, D. Q., *et al.* (2018) A novel strain of Porcine deltacoronavirus in Vietnam. *Arch. Virol.* **163**, 203–207
3. Zhao, Y., Qu, H., Hu, J., Fu, J., Chen, R., Li, C., *et al.* (2019) Characterization and pathogenicity of the Porcine deltacoronavirus isolated in southwest China. *Viruses* **11**, 1074
4. Li, B., Zheng, L., Li, H., Ding, Q., Wang, Y., and Wei, Z. (2019) Porcine deltacoronavirus causes diarrhea in various ages of field-infected pigs in China. *Biosci. Rep.* **39**, BSR20190676
5. Jung, K., Hu, H., and Saif, L. J. (2017) Calves are susceptible to infection with the newly emerged Porcine deltacoronavirus, but not with the swine enteric alphacoronavirus, porcine epidemic diarrhea virus. *Arch. Virol.* **162**, 2357–2362
6. Zhang, H., Ding, Q., Yuan, J., Han, F., Wei, Z., and Hu, H. (2022) Susceptibility to mice and potential evolutionary characteristics of Porcine deltacoronavirus. *J. Med. Virol.* **94**, 5723–5738
7. Boley, P. A., Alhamo, M. A., Lossie, G., Yadav, K. K., Vasquez-Lee, M., Saif, L. J., *et al.* (2020) Porcine deltacoronavirus infection and transmission in poultry, United States(1). *Emerg. Infect. Dis.* **26**, 255–265

8. Lednicky, J. A., Tagliamonte, M. S., White, S. K., Elbadry, M. A., Alam, M. M., Stephenson, C. J., *et al.* (2021) Independent infections of Porcine deltacoronavirus among Haitian children. *Nature* **600**, 133–137
9. Wißing, M. H., Brüggemann, Y., Steinmann, E., and Todt, D. (2021) Virus-host cell interplay during Hepatitis E virus infection. *Trends Microbiol.* **29**, 309–319
10. de Wilde, A. H., Snijder, E. J., Kikkert, M., and van Hemert, M. J. (2018) Host factors in coronavirus replication. *Curr. Top. Microbiol. Immunol.* **419**, 1–42
11. Yang, Y. L., Liu, J., Wang, T. Y., Chen, M., Wang, G., Yang, Y. B., *et al.* (2021) Aminopeptidase N is an entry co-factor triggering Porcine deltacoronavirus entry via an endocytotic pathway. *J. Virol.* **95**, e0094421
12. Zhu, X., Liu, S., Wang, X., Luo, Z., Shi, Y., Wang, D., *et al.* (2018) Contribution of porcine aminopeptidase N to Porcine deltacoronavirus infection. *Emerg. Microbes Infect.* **7**, 65
13. Li, W., Hulswit, R. J. G., Kenney, S. P., Widjaja, I., and Bosch, B.-J. (2018) Broad receptor engagement of an emerging global coronavirus may potentiate its diverse cross-species transmissibility. *Proc. Natl. Acad. Sci. U. S. A.* **115**, E5135–E5143
14. Li, S., Xiao, D., Zhao, Y., Zhang, L., Chen, R., Liu, W., *et al.* (2022) Porcine deltacoronavirus (PDCoV) entry into PK-15 cells by caveolae-mediated endocytosis. *Viruses* **14**, 496
15. Fang, P., Zhang, J., Zhang, H., Xia, S., Ren, J., Tian, L., *et al.* (2021) Porcine deltacoronavirus enters porcine IPI-2I intestinal epithelial cells via macropinocytosis and clathrin-mediated endocytosis dependent on pH and dynamin. *J. Virol.* **95**, e0134521
16. Ji, H. J., and Lee, C. (2018) Cholesterol is important for the entry process of Porcine deltacoronavirus. *Arch. Virol.* **163**, 3119–3124
17. Ke, W., Wu, X., Fang, P., Zhou, Y., Fang, L., and Xiao, S. (2021) Cholesterol 25-hydroxylase suppresses Porcine deltacoronavirus infection by inhibiting viral entry. *Virus Res.* **295**, 198306
18. Qu, H., Wen, Y., Hu, J., Xiao, D., Li, S., Zhang, L., *et al.* (2022) Study of the inhibitory effect of STAT1 on PDCoV infection. *Vet. Microbiol.* **266**, 109333
19. Sun, L., Zhao, C., Fu, Z., Fu, Y., Su, Z., Li, Y., *et al.* (2021) Genome-scale CRISPR screen identifies TMEM41B as a multi-function host factor required for coronavirus replication. *PLoS Pathog.* **17**, e1010113
20. Zhu, Y., Feng, F., Hu, G., Wang, Y., Yu, Y., Zhu, Y., *et al.* (2021) A genome-wide CRISPR screen identifies host factors that regulate SARS-CoV-2 entry. *Nat. Commun.* **12**, 961
21. Zhu, S., Liu, Y., Zhou, Z., Zhang, Z., Xiao, X., Liu, Z., *et al.* (2021) Genome-wide CRISPR activation screen identifies candidate receptors for SARS-CoV-2 entry. *Sci. China Life Sci.* **65**, 701–717
22. Wei, J., Alfajaro, M. M., DeWeirdt, P. C., Hanna, R. E., Lu-Culligan, W. J., Cai, W. L., *et al.* (2021) Genome-wide CRISPR screens reveal host factors critical for SARS-CoV-2 infection. *Cell* **184**, 76–91.e13
23. Kratzel, A., Kelly, J. N., V'Kovski, P., Portmann, J., Brüggemann, Y., Todt, D., *et al.* (2021) A genome-wide CRISPR screen identifies interactors of the autophagy pathway as conserved coronavirus targets. *PLoS Biol.* **19**, e3001490
24. Baggen, J., Persoons, L., Vanstreels, E., Jansen, S., Van Looveren, D., Boeckx, B., *et al.* (2021) Genome-wide CRISPR screening identifies TMEM106B as a proviral host factor for SARS-CoV-2. *Nat. Genet.* **53**, 435–444
25. Wang, R., Simoneau, C. R., Kulsuptrakul, J., Bouhaddou, M., Travisano, K. A., Hayashi, J. M., *et al.* (2021) Genetic screens identify host factors for SARS-CoV-2 and common cold coronaviruses. *Cell* **184**, 106–119.e14
26. Luo, Y., Tan, C. W., Xie, S.-Z., Chen, Y., Yao, Y.-L., Zhao, K., *et al.* (2021) Identification of ZDHHC17 as a potential drug target for Swine acute diarrhea syndrome coronavirus infection. *mBio* **12**, e0234221
27. Tse, L. V., Meganck, R. M., Araba, K. C., Yount, B. L., Shaffer, K. M., Hou, Y. J., *et al.* (2022) Genomewide CRISPR knockout screen identified PLAC8 as an essential factor for SADS-CoVs infection. *Proc. Natl. Acad. Sci. U. S. A.* **119**, e2118126119
28. Richardson, R. B., Ohlson, M. B., Eitson, J. L., Kumar, A., McDougal, M. B., Boys, I. N., *et al.* (2018) A CRISPR screen identifies IFI6 as an ER-resident interferon effector that blocks flavivirus replication. *Nat. Microbiol.* **3**, 1214–1223
29. Li, C., Chu, H., Liu, X., Chiu, M. C., Zhao, X., Wang, D., *et al.* (2020) Human coronavirus dependency on host heat shock protein 90 reveals an antiviral target. *Emerg. Microbes Infect.* **9**, 2663–2672
30. Zhao, Z., Xu, L. D., Zhang, F., Liang, Q. Z., Jiao, Y., Shi, F. S., *et al.* (2023) Heat shock protein 90 facilitates SARS-CoV-2 structural protein-mediated virion assembly and promotes virus-induced pyroptosis. *J. Biol. Chem.* **299**, 104668
31. Zhang, S., Huang, W., Ren, L., Ju, X., Gong, M., Rao, J., *et al.* (2022) Comparison of viral RNA-host protein interactomes across pathogenic RNA viruses informs rapid antiviral drug discovery for SARS-CoV-2. *Cell Res.* **32**, 9–23
32. Wyler, E., Mösbauer, K., Franke, V., Diag, A., Gottula, L. T., Arsiè, R., *et al.* (2021) Transcriptomic profiling of SARS-CoV-2 infected human cell lines identifies HSP90 as target for COVID-19 therapy. *iScience* **24**, 102151
33. Stoian, A., Rowland, R. R. R., Petrovan, V., Sheahan, M., Samuel, M. S., Whitworth, K. M., *et al.* (2020) The use of cells from ANPEP knockout pigs to evaluate the role of aminopeptidase N (APN) as a receptor for Porcine deltacoronavirus (PDCoV). *Virology* **541**, 136–140
34. Zhao, Y., Xiao, D., Zhang, L., Song, D., Chen, R., Li, S., *et al.* (2022) HSP90 inhibitors 17-AAG and VER-82576 inhibit Porcine deltacoronavirus replication in vitro. *Vet. Microbiol.* **265**, 109316
35. Bolhassani, A., and Agi, E. (2019) Heat shock proteins in infection. *Clin. Chim. Acta* **498**, 90–100
36. Ma, R., Zhang, Y., Liu, H., and Ning, P. (2014) Proteome profile of swine testicular cells infected with porcine transmissible gastroenteritis coronavirus. *PLoS One* **9**, e110647
37. Reyes-Del Valle, J., Chávez-Salinas, S., Medina, F., and Del Angel, R. M. (2005) Heat shock protein 90 and heat shock protein 70 are components of dengue virus receptor complex in human cells. *J. Virol.* **79**, 4557–4567
38. Seo, H. W., Seo, J. P., and Jung, G. (2018) Heat shock protein 70 and heat shock protein 90 synergistically increase Hepatitis B viral capsid assembly. *Biochem. Biophys. Res. Commun.* **503**, 2892–2898
39. Sakata, M., Katoh, H., Otsuki, N., Okamoto, K., and Mori, Y. (2019) Heat shock protein 90 ensures the integrity of Rubella virus p150 protein and supports viral replication. *J. Virol.* **93**, e01142-19
40. Zhang, W. J., Wang, R. Q., Li, L. T., Fu, W., Chen, H. C., and Liu, Z. F. (2021) Hsp90 is involved in Pseudorabies virus virion assembly via stabilizing major capsid protein VP5. *Virology* **553**, 70–80
41. Purnima, K., Pratibha, G., Rashmi, K., and Lal, S. K. (2019) Influenza A virus neuraminidase protein interacts with Hsp90, to stabilize itself and enhance cell survival. *J. Cell. Biochem.* **120**, 6449–6458
42. Roby, J. A., Esser-Nobis, K., Dewey-Verstelle, E. C., Fairgrieve, M. R., Schwerk, J., Lu, A. Y., *et al.* (2020) Flavivirus nonstructural protein NS5 dysregulates HSP90 to broadly inhibit JAK/STAT signaling. *Cells* **9**, 899
43. Liu, D., Wu, A., Cui, L., Hao, R., Wang, Y., He, J., *et al.* (2014) Hepatitis B virus polymerase suppresses NF-κB signaling by inhibiting the activity of IKKs via interaction with Hsp90β. *PLoS One* **9**, e91658
44. Masters, P. S., and Sturman, L. S. (1990) Background paper. Functions of the coronavirus nucleocapsid protein. *Adv. Exp. Med. Biol.* **276**, 235–238
45. Ding, Z., Luo, S., Gong, W., Wang, L., Ding, N., Chen, J., *et al.* (2020) Subcellular localization of the Porcine deltacoronavirus nucleocapsid protein. *Virus Genes* **56**, 687–695
46. Lee, S., and Lee, C. (2015) Functional characterization and proteomic analysis of the nucleocapsid protein of Porcine deltacoronavirus. *Virus Res.* **208**, 136–145
47. Choi, S., and Lee, C. (2019) Functional characterization and proteomic analysis of Porcine deltacoronavirus accessory protein NS7. *J. Microbiol. Biotechnol.* **29**, 1817–1829
48. Fang, P., Hong, Y., Xia, S., Zhang, J., Ren, J., Zhou, Y., *et al.* (2021) Porcine deltacoronavirus nsp10 antagonizes interferon-β production independently of its zinc finger domains. *Virology* **559**, 46–56
49. Ji, L., Wang, N., Ma, J., Cheng, Y., Wang, H., Sun, J., *et al.* (2020) Porcine deltacoronavirus nucleocapsid protein species-specifically suppressed IRF7-induced type I interferon production via ubiquitin-proteasomal degradation pathway. *Vet. Microbiol.* **250**, 108853
50. Genest, O., Wickner, S., and Doyle, S. M. (2019) Hsp90 and Hsp70 chaperones: collaborators in protein remodeling. *J. Biol. Chem.* **294**, 2109–2120

51. Katoh, H., Kubota, T., Nakatsu, Y., Tahara, M., and Takeda, M. (2017) Heat shock protein 90 ensures efficient mumps virus replication by assisting with viral polymerase complex formation. *J. Virol.* **91**, e02220-16
52. Massey, A. J., Williamson, D. S., Browne, H., Murray, J. B., Dokurno, P., Shaw, T., *et al.* (2010) A novel, small molecule inhibitor of Hsc70/Hsp70 potentiates Hsp90 inhibitor induced apoptosis in HCT116 colon carcinoma cells. *Cancer Chemother. Pharmacol.* **66**, 535–545
53. Scherer, M., Klingl, S., Sevvana, M., Otto, V., Schilling, E. M., Stump, J. D., *et al.* (2014) Crystal structure of cytomegalovirus IE1 protein reveals targeting of TRIM family member PML via coiled-coil interactions. *PLoS Pathog.* **10**, e1004512
54. Fu, J., Chen, R., Hu, J., Qu, H., Zhao, Y., Cao, S., *et al.* (2020) Identification of a novel linear B-cell epitope on the nucleocapsid protein of Porcine deltacoronavirus. *Int. J. Mol. Sci.* **21**, 648
55. Reed, L. J., and Muench, H. (1938) A simple method of estimating fifty per cent endpoints12. *Am. J. Epidemiol.* **27**, 493–497